BUCKEYE VERTICAL
AT THE OHIO STATE UNIVERSITY®

Vertical Flight Society

2021 –2022 Design-Build-Vertical Flight Competition

Final Technical Report

May 2nd, 2022

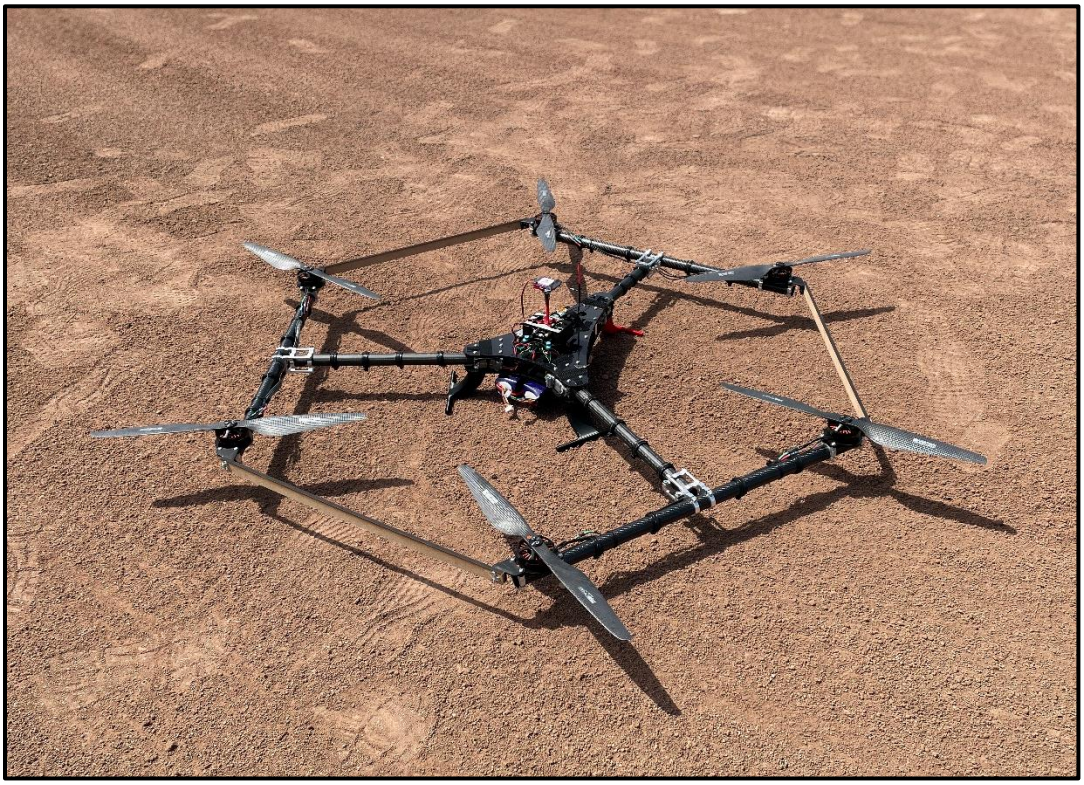

Executive Summary

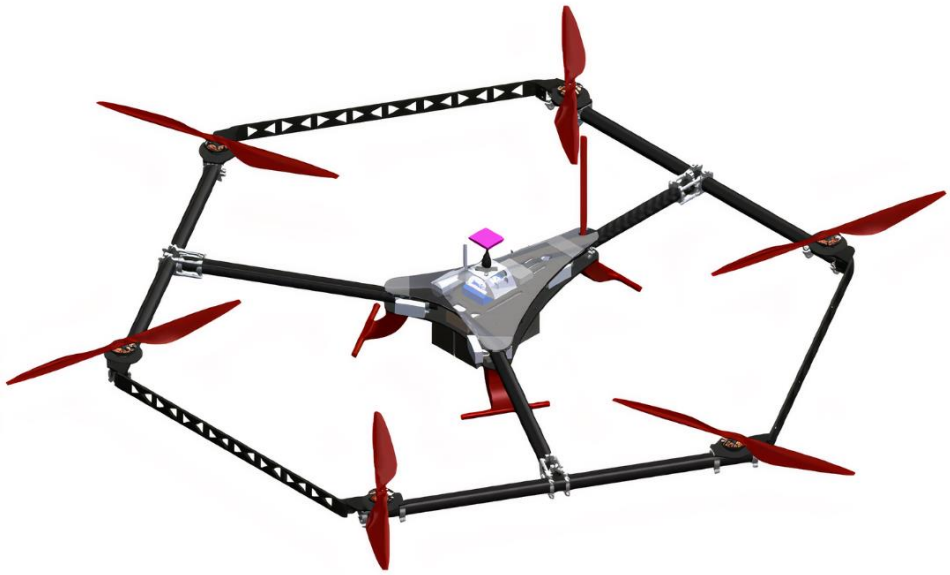

Figure 1: Buckeye Vertical CAD Model of Aircraft

Buckeye Vertical (BV), a student organization at The Ohio State University (OSU), was founded in the Fall of 2020 to create a platform for students to explore Advanced Air Mobility (AAM) and Uncrewed Aircraft Systems (UAS). One of Buckeye Vertical's main goals is to give students the opportunity to explore and understand this field of study through professional development opportunities and project-based competitions that will support and create a platform of academic enrichment and excellence. AAM is a rapidly growing field and Buckeye Vertical strives to spread awareness and engage the student community in a variety of ways regarding vertical flight technology. Buckeye Vertical is competing in the 2021-2022 Vertical Flight Society's (VFS) Design-Build-Vertical Flight (DBVF) student competition. The goal is to develop an aircraft that successfully meets the Request for Proposal (RFP) requirements while providing students with hands-on experience in electric vertical take-off and landing (eVTOL) technology.

The objective is to design an eVTOL UAS aircraft that is a subscale model for an AAM aircraft that can take off and land vertically and transition between vertical and forward flight while developing a report to document the engineering design challenges, technical intricacies, and decisions approached throughout the project. The maximum takeoff weight, including a payload of a minimum of 2 lb., must not exceed 15 lb. The aircraft additionally must be within 6.5 feet across, provide a shunt plug 6 inches away from the rotors with the ability to arm and disarm the aircraft's power system, contain a separate power source for the flight control system, and follow the U.S. Federal Communications Commission Part 15 rules for transmission frequencies and International Telecommunication Union Region 2 frequency allocations.

Buckeye Vertical aimed to build a unique team of individuals, which includes a variety of disciplines and class standings. The versatility in background enabled the team to design, construct, and test an eVTOL aircraft to meet the specific challenges set forth by the competition Goals were set to achieve maximum scoring such as the aircraft's flight time, payload capacity, and power efficiency. The team began to set design requirements to understand minimum thrust and aircraft weight, required power draw, and motor/propeller configurations that would yield a 10-minute flight time with maximized payload capacity. Various UAS configurations were considered, and the team narrowed the selection to three final configuration concepts: quadcopter, hexacopter, and octocopter. The team chose to design and build a hexacopter after evaluating the design requirements of each configuration with the performance challenges using a house of quality table. The team was sub-divided into two groups, Avionics and Structures, to work on the aircraft in parallel and synergize the output of each sub-team.

The Avionics sub-team explored various propulsion and power system components in conjunction with the aircraft requirements to determine an optimized propulsion system. Propulsion systems including motors, propellers, and batteries were down selected on their performance with a maximum flight time and aircraft weight. Two Tattu 6S lithium polymer batteries were selected along with a T-Motor's Antigravity MN5008 340KV motor. Based on manufacturer's recommendation, 18x6.1 size propellers and 40 Amp electronic speed controllers were chosen. A separate 2s battery was utilized to power the flight controller. Once the aircraft was assembled, the team iteratively improved the vibration of the frame so the vehicle can be tuned for maximum stability and ease of autonomous flight. The auto-tune feature within the PX4 firmware was referenced for the initial tuning, after which manual changes were performed based on the flight

performance. Multiple flight tests with varying airframe and payload weight were performed to compare flight time and performance. A sample quadcopter was assembled to test and validate the autonomous mission plans prior to testing it in the actual aircraft.

The Structures sub-team developed initial CAD models of the aircraft and iterated the design based on frequent feedback from discussions between both sub-teams. As the CAD model of the aircraft was iterated, manufacturing processes were explored and estimates on purchasing critical components were completed to ensure high-demand items were ordered in advance to mitigate supply-chain delays. An emphasis was put on utilizing composites to help strengthen subassemblies of the vehicle, while keeping the weight to a minimum. Once the first version of the aircraft was assembled, the team iteratively improved the vibration of frame, tuned the vehicle for maximum stability and ease of autonomous flight.

The aircraft design was validated through flight testing, and a 20-minute hover time was achieved. The hover time matched predictions, however, the efficiency of the motors is expected to drop during forward flight. The team will continue to flight test leading to the in-person competition. Between the submission of the Final Technical Report and the in-person fly-off in June, the autonomy testing and full-scale practice flights of the mapped-out course will be completed to prepare for the competition.

Management Summary

The Buckeye Vertical Competition Team for the 2021 to 2022 academic year was broken into two technical sub-teams: avionics and structures. The team, majority of whom are underclassmen, consists of a diverse range of engineering disciplines including aerospace, mechanical, physics, and electrical. Among the 18 undergraduate student members, a student was appointed to be the designated lead for each sub-team, with each sub-team containing a mixture of members and additional leads. The avionics sub-team is responsible for developing the control system of the aircraft and contains the software lead, propulsion lead, and flight test lead. The structures sub-team is responsible for designing and developing the structural design and aircraft frame, including the assembly and integration of all components and connection of all subsystems. The structures sub-team includes the design lead, structural analysis lead, and aerospace lead. An equipment manager is responsible for communicating with each sub-team to curate and manage all materials that need to be purchased. The team lead is responsible for the direction of overall team activities, communication between both sub-teams, advisor relations, and budget management. View Figure 2 for overall team organization and Figure 3 below for the competition team schedule.

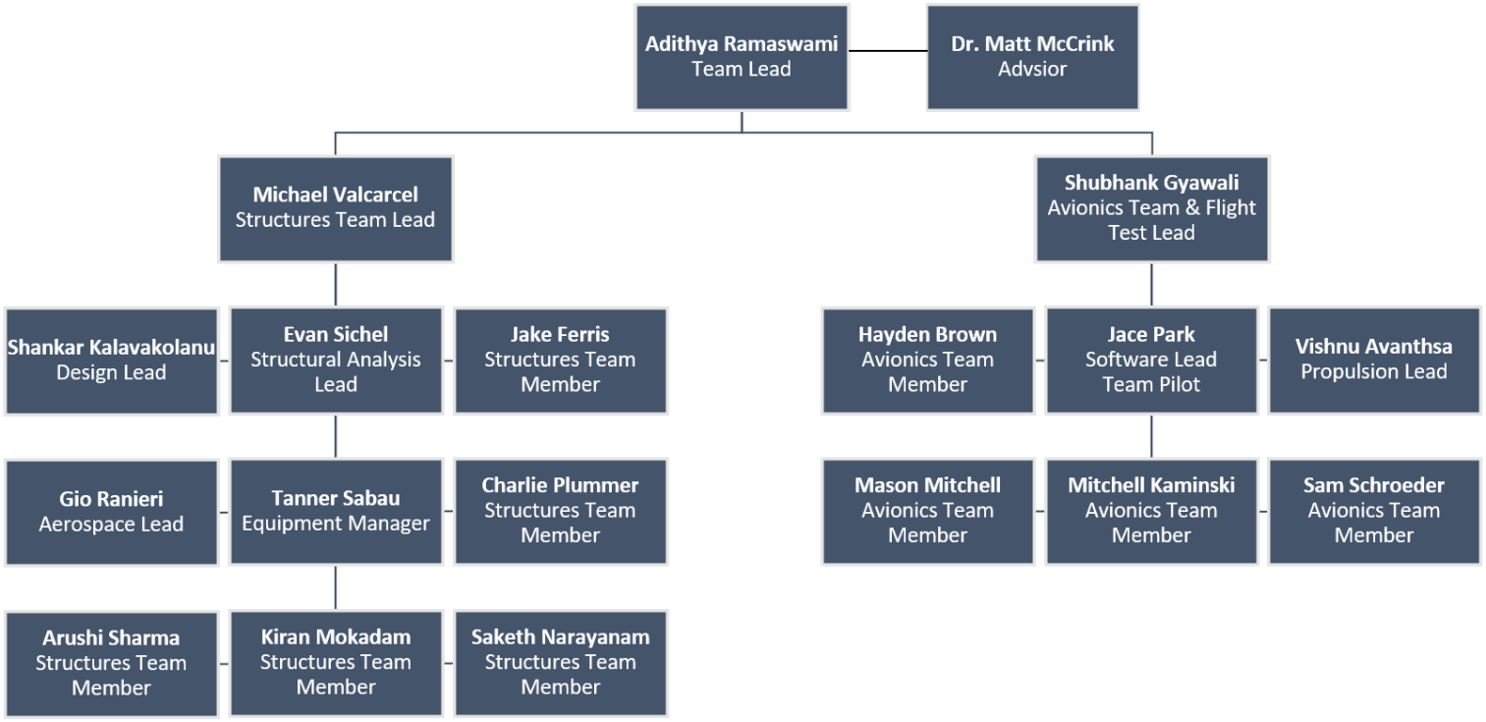

Figure 2: Buckeye Vertical Competition Team Organization Chart

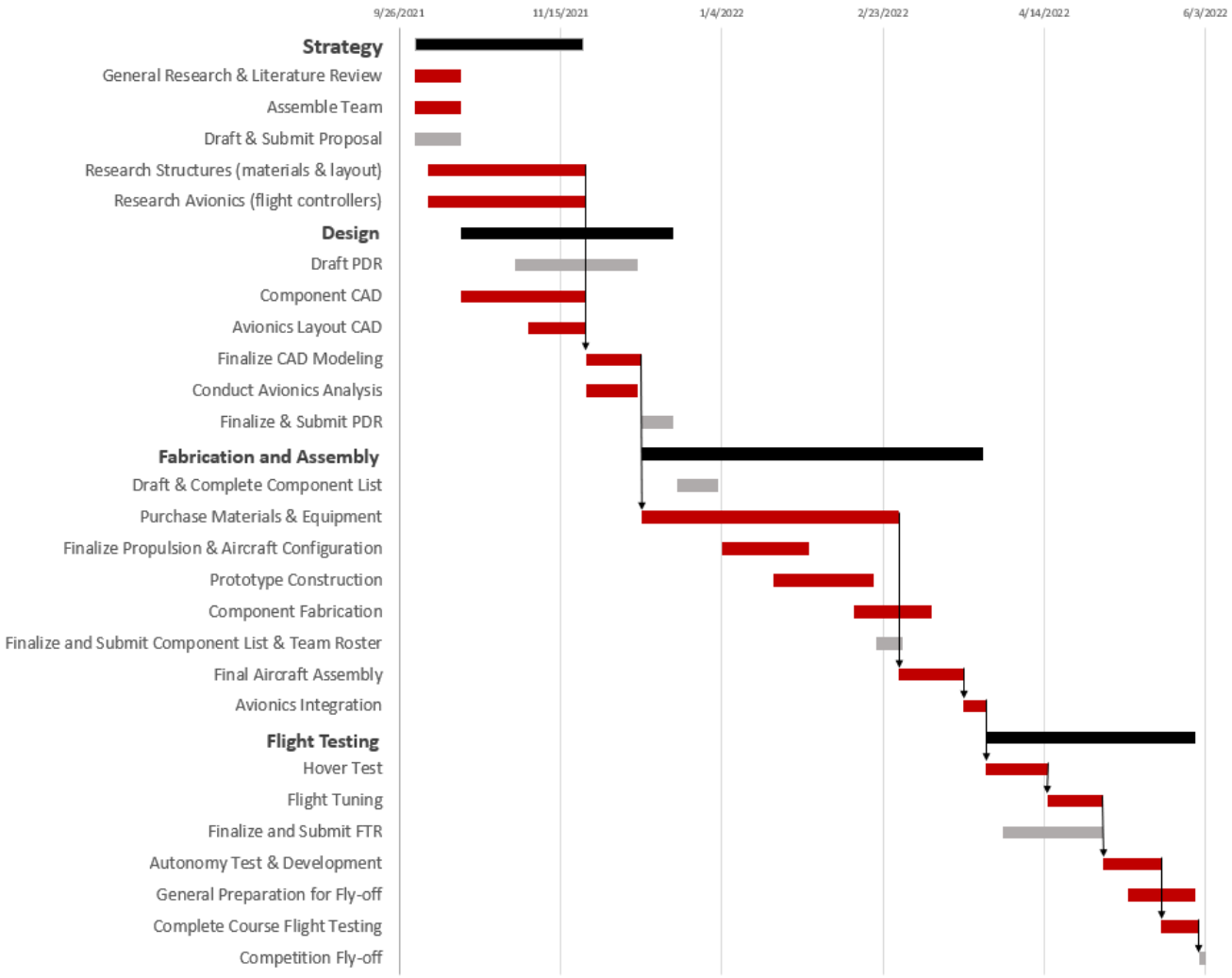

Figure 3: Team Gantt Chart for the 2021-2022 Project Cycle

Design Trade Studies

Design Drivers

The fly-off competition focuses on four main categories: range, speed, payload capacity, and autonomy. These are measured through four challenges, which assess: the number of laps completed on a given course, the fastest time to complete three laps, the payload capacity, and completion of the autonomous flight portion. The mission scoring rubric was considered to select a final configuration that scored the most points during the fly-off portion.

For manual missions, the aircraft will complete laps in the shortest amount of time possible around the Flight Performance Course. Starting at the VTOL zone, the aircraft will lift off approximately 5 feet from the ground and land 4 separate times at each respective zone to complete a lap. This process will be repeated for three laps for the Flight Performance Course scoring section, which includes 50 possible points for the fastest time. After the three initial laps are finished, the aircraft will continue to complete as many laps as possible to score an additional 50 points for most laps done at the end of 10 minutes. The final 50 possible points are given based on the aircraft's payload fraction scoring. This objective requires the aircraft to maximize its speed, agility, take-off and landing efficiency, endurance, and payload. Altogether, the manual portion of the fly-off totals 150 points, which is 50% of the maximum fly-off score.

The autonomous mission encompasses the remaining portion of the fly-off scoring. The same course that is utilized for manual piloting is used for autonomous flights. An aircraft with successful completion of the autonomy course receives 150 points, while incompletion is 0 points. In addition to the requirements needed for the manual missions, the execution of the autonomy course will require the aircraft to maximize stability, flight time, and ease of automation. The aircraft's performance will also require simple and precise control for accurate take-off and landing procedures.

Aircraft Configuration Selection Process

To maximize scoring in the fly-off portion, the aircraft needs high speed, agility, and payload capacity while following the competition requirements of flying for 10 minutes and weighing less than 15 lb. To achieve this, a design matrix was created to compare configurations using design parameter factors determined by the competition scoring rubric.

Table 1: Design Matrix

Design Parameters (Weight)	Quadcopter	Hexacopter	Co-axial Quadcopter	Fixed Wing 4-Prop Tilt-Rotor	Octocopter
Flight Time (5)	43	45	28	37	35
Overall Stability (4)	36	41	42	31	44
Power Efficiency (5)	37	45	40	40	40
Size (2)	40	37	40	34	34
Weight (4)	46	43	42	37	31
Speed (4)	40	46	47	48	46
Acceleration/Deceleration (5)	43	46	48	45	47
Manufacturability (3)	47	47	45	38	47
Simplicity (3)	46	45	34	32	44
Payload Capacity (5)	32	42	41	40	44
Ease of Automation (5)	41	44	35	31	45
Score	182.7	***198***	180.1	170.7	188

Five main aircraft configurations were compared for their estimated performance on the fly-off portions utilizing the design matrix above. The design parameters and their respective weights were determined by their correlation to the possible points given on the scoring rubric. The individual cell scores were determined after researching articles discussing and comparing the unique configurations within each category [1], respectively. The parameters with higher weights were determined to be more important for the competition objectives. A target aircraft weight of 15 lb. including payload was assumed while performing the comparison among aircraft configurations.

In addition, each cell was given a corresponding color. A characteristic that a specific configuration excelled in was shaded green and a characteristic that was seen as a disadvantage was shaded red. After evaluating the results from the design matrix, three configurations were deemed favorable based on the competition requirements: quadcopter (4-prop), hexacopter (6-prop), and octocopter (8-prop).

Final Aircraft Configuration Selection

A comparison of the highest performing aircraft configurations led to the final aircraft selection. To make the comparison fair, the team assumed an optimized motor and propeller configuration that allows the final 3 aircraft configurations to have enough force to lift aircraft and at least 10 minutes of flight time from the batteries. With these constants enforced, the team compared parameters including payload fraction, speed, acceleration, ease of maneuverability, and stability. The quadcopter excelled in size and simplicity due to its basic four-arm rotor design. However, it was predicted to perform poorly on payload capacity and stability because of low thrust output in comparison to the other configurations. The octocopter was another configuration that had a high relative score on the design matrix due to its stability, ease of automation, and payload capacity. The octocopter excelled in these categories of the competition fly-off because of the high thrust output from the eight rotors. However, the octocopter had low predicted performance in weight and size.

The hexacopter configuration was selected as the final aircraft design for its high performance in rapid acceleration in all directions due to a high thrust to weight ratio, moderately high payload fraction, stability, and ease of automation. This results from the balance between high relative thrust and stability for automated flight from six rotors. The only parameters that the hexacopter lacked were size and the payload capacity in comparison to a quadcopter and octocopter, respectively.

Propulsion Selection Process

The avionic component selection process began with the assumption that the drone would weigh 15 lb. and need to hover at 50% thrust. The flight performance course scoring favors both high payload fractions and endurance, thus a large thrust-to-weight ratio is necessary to optimize the hexacopter's performance in these sections. The manufacturer provided data for a broad range of motor and propellor configurations, which was then narrowed down by targeting configurations that produced between 2.2-3.3 lb. of thrust at 50% thrust. Since each battery is limited to 100 WH, two 6s batteries in parallel were selected as it is within the competition limit. To fit within the maximum dimensions allowed by competition rules, the hexacopter's propeller diameter was limited to 20 inches. A MATLAB application was written to calculate aircraft thrust and component weights based on equation relations presented by C. Ampatis addressing optimal component selection in multirotor vehicles [2]. The calculated weight and thrust outputs, combined with structure and competition limitations narrowed the options to 15 potential configurations.

Following the mass parametrization step, the 15 motor-propeller combinations that passed into the next phase were then analyzed using eCalc, a web-based motor drive calculator. Using this software, the estimated ranges and corresponding flight times for each of the motor-propeller configurations were calculated [3]. All configuration calculations were based on a hexacopter with a total weight of 15 lb., which included a payload of approximately 2 - 4 lb. The field conditions were set to resemble the Army Research Lab's elevation (259.2 ft.ASL), predicted air temperature (78.8 °F), and predicted air pressure (1004 hPa) during the week of the competition. With these parameters in place, the predicted endurance calculations lead to the determination that the optimal configuration for the propulsion systems for the hexacopter design would be the T-MOTOR Antigravity MN5008 KV340 coupled with the T-MOTOR P18*6.1" CF propellers.

Technical Innovations

Evolution of the Prosthetic Leg-Inspired Landing Gear

Landing Gear Version 1

After researching landing gear options, a decision was made to incorporate a biomedical design reflecting that of a prosthetic leg. Considering the possibility of the normal force acting anywhere along the bottom of the curve being like that of a person walking, the prosthetic leg design accounts for the variability of any deviations from the optimal landing angle, along with reducing the stress applied at a given point by spreading the load. When looking at the flight competition requirements, the aircraft is required to take off and land over 40 times. With this, a durable and springy landing gear will help reduce the amount of stress put on the main airframe. To prove the functionality of this design, the stress and deflection requirements of the landing gear must be determined. The worst-case scenario of crashing the aircraft from a 7 feet height free fall was utilized to ensure the maximum force the potential landing gear would face.

The displacement and stress results of this force were modeled through SolidWorks seen in Figure 4 on the following page. With the maximum force of 48.8 lb. per landing gear, the maximum displacement was 2.36 in, with the highest stress point having $1.75 * 10^4$ lb/in^2 of force being applied.

Landing Gear Version 2

The primary issue with the first iteration landing gear was the natural frequency vibration caused by the spring-like landing gear attempting to balance the weight of the aircraft during landing. The original design was created with the intent to absorb the force of the ground. However, this intention was overcompensated for and led to a large lapse in time for the aircraft to come to a complete stop. The reason this led to concern is the rule stating the aircraft may not translate in motion to complete a satisfactory touchdown. The second iteration of the landing gear was adapted to mitigate the system's vibration by incorporating a more rigid body. To overcome this problem, a new landing gear was created with more stability and a thicker structure. The second iteration cut down the time to a complete stop which in turn optimizes scoring.

Landing Gear Version 3

The third iteration of the landing gear was needed due to the second version's inability to overcome the force of moderate landings causing it to crack at the sharp edge near the fixed end. Since this edge is at the peak of the stress curve, the bending and shear stress is maximized at this location. Due to the shear stress applied when the aircraft falls, the landing gear would break at this edge. While testing the aircraft, this theoretical application was proven to be true while the hexacopter fell from a moderate height. After careful observation of the break in the landing gear, it was determined that the break occurred at the threshold of the sharp edge. To overcome this issue, a two-front approach was taken. First, the sharp edge of the design was eliminated altogether using fillets at any sharp edge. Secondly, the height of the landing gear was decreased to limit the moment arm applied to the landing gear. The prosthetic leg like curve was thickened to ensure the landing gear would sustain the force on impact with the ground while still limiting the vibration experienced. The adjustments from iteration one to iteration three were implemented to simplify the design, guarantee structure stability, and limit vibration to the aircraft. Refer to Figure 4 below to see the evolution of landing gear.

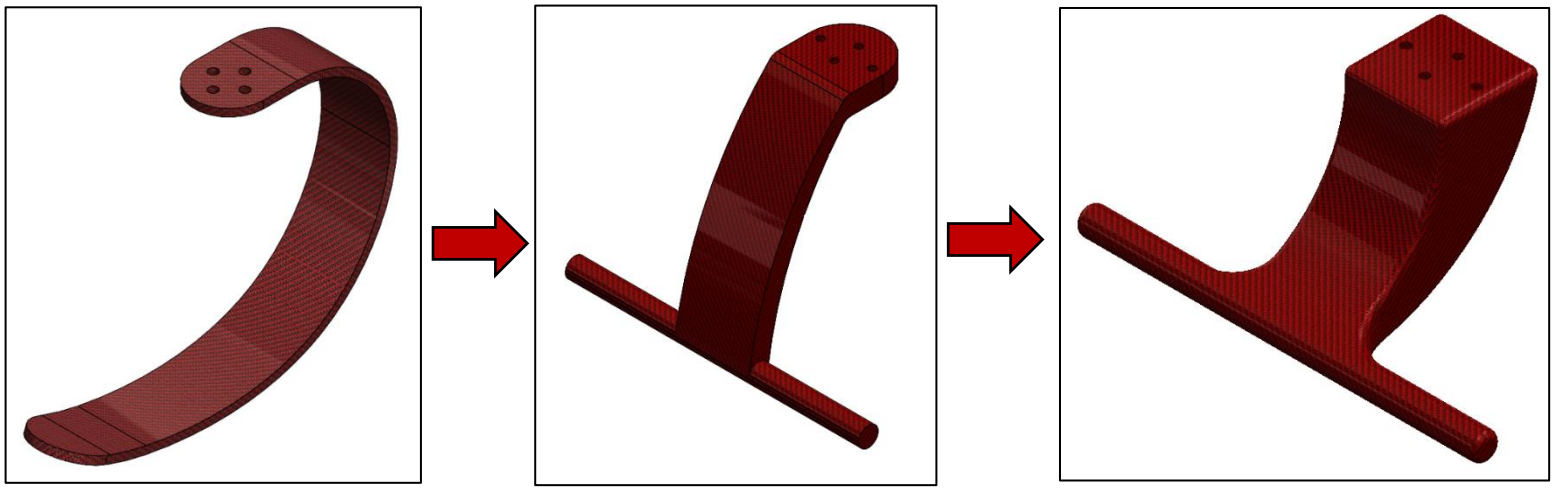

Landing Gear Version 1 **Landing Gear Version 2** **Landing Gear Version 3**

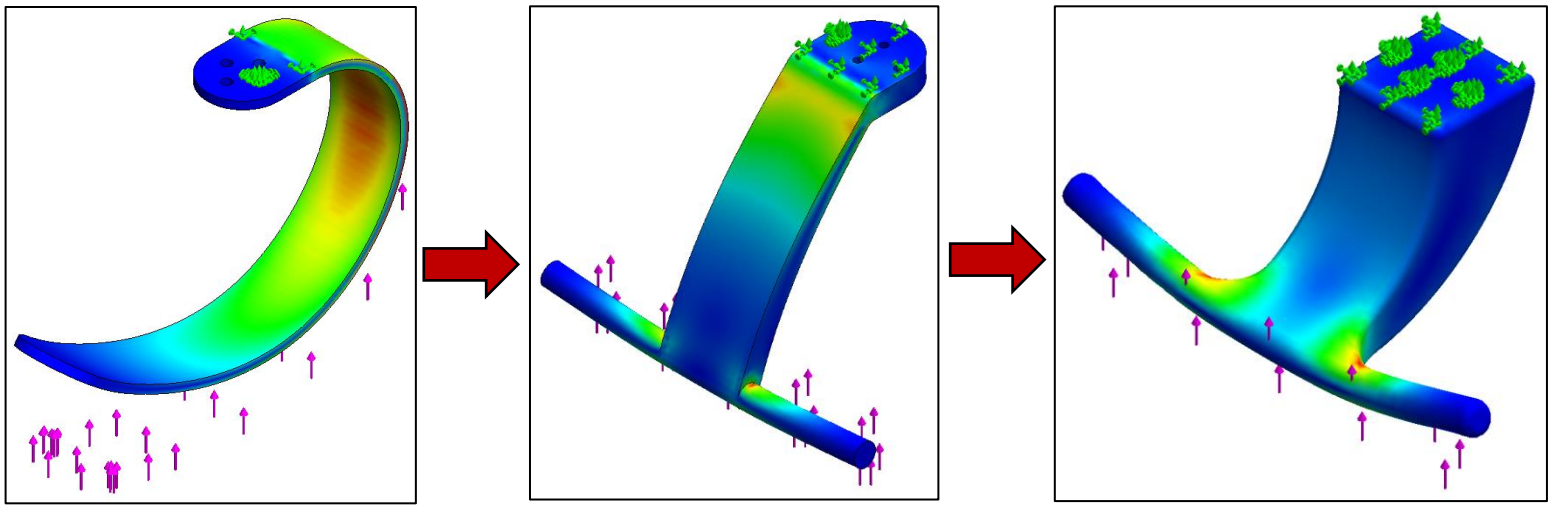

Maximum Stress: $8.2 * 10^8\ N/m^2$ **Maximum Stress:** $1.4 * 10^7\ N/m^2$ **Maximum Stress:** $8.9 * 10^5\ N/m^2$

Figure 4: Evolution of landing gear shape and stress results

Triple T-Arm Design

Figure 5: Single T-Arm Assembly

After the hexacopter configuration was selected, a conventional hexacopter design using six arms radiating from the fuselage was considered. While this is the simplest possible overall design, the attachment points for the arms are bulky compared to the size of the fuselage. When multiplied by six, this causes high material costs and complexity in the fuselage design. The team addressed this issue by innovating a Triple T-Beam design that contains 3 radial tubes attached to the center fuselage. Additionally, 3 tangentially oriented tubes are inserted to the ends of each radial tube and hold a motor and propeller at each end. This creates a "T" shape (shown in Figure 5) with each of the 3 "T"s oriented radially outwards. This allows the usage of 6 motors like a conventional hexacopter but reduces fuselage complexity including more space for avionics and payload. The detailed benefits and drawbacks for the Triple T-Arm design compared to a traditional radial hexacopter are shown in Table 2 below.

Table 2: Benefits and Drawbacks of Triple T-Arm Design compared to Traditional Radial Hexacopter

Benefits	Drawbacks
Greater access to fuselage	Large torsional force present at fixed end of radial tubes
20% reduction in weight	Extra vibrations caused by motor alignment difficulties
35% reduction in material cost	

This design presented a challenge. When the motors on either end of the tangential tubes produced asymmetrical thrust, torsion was caused around the radial tubes. This could change propeller direction enough to cause flight instability through internal vibrations. To combat this, the radial tubes were down selected using moment of inertia calculations to identify a proper carbon fiber tube diameter and wall thickness that would resist the tendency to twist due to the torsion produced by the varying thrusts of the motors on each end of the T-Arms. 10 tubes were analyzed using inputs such as outer diameter, inner diameter, wall thickness, weave pattern, bending strength, and mass provided by the supplier's specifications. From there, the moment of inertia and maximum allowable stress were calculated for each of the selected tubes.

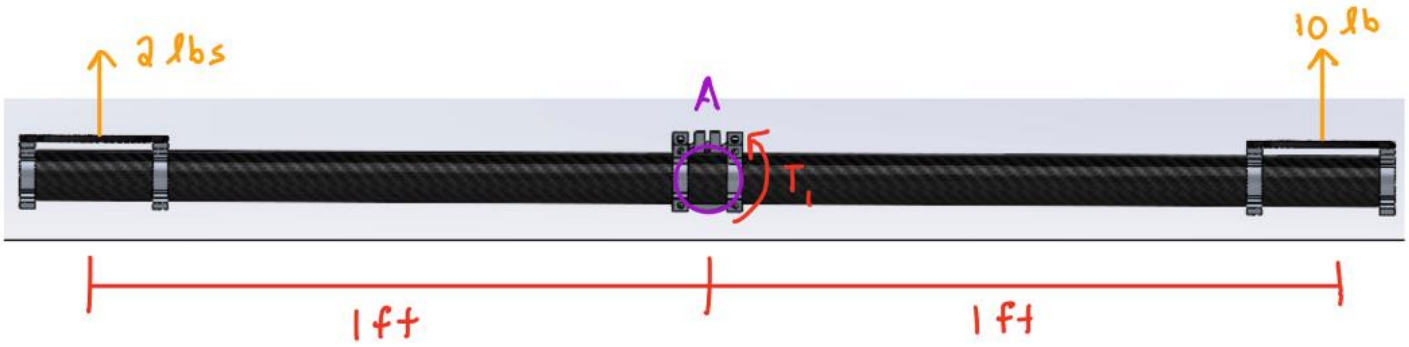

Figure 6: Free Body Diagram of Single T-Arm

A free body diagram shown above was created to calculate the maximum torsional force. This maximum force would occur when the two motors attached to each end produced different thrust to complete pitch, roll, and yaw maneuvers. The maximum stress present from the torsional force was calculated to be 15,000 Pa. With a factor of safety of 1.2 implemented the maximum stress estimated is 18,000 Pa. The team selected a 1-inch outer diameter tube that would be compatible with the fastening clamp hubs and a wall thickness of .036 inch that had a maximum allowable stress of 20,000 Pa. Also, the pultruded carbon fiber pattern weave was selected for the radial tubes due to its higher resistance to torsion among the other weaves. In addition, because the tubes on the physical aircraft have no fixed attachment points, aligning the motors is difficult. The asymmetrical thrust from misalignment could cause instability. To prevent this, the beam orientations were carefully aligned using an electronic level at each of the motors.

Despite its shortcomings, the aircraft gained performance from a lighter, smaller, more spacious, and more aerodynamically efficient fuselage. The tubes were built stiff enough and adjusted precisely enough to achieve stable flight. Overall, the design achieves mission objectives with less fuselage structure.

Mission Model

The hover thrust for each motor of the 12.125 lb. hexacopter aircraft is around 2.028 lb. which corresponds to 40% throttle value of our propulsion system. Since the aircraft tilts forward to create horizontal thrust, the throttle value is approximately 55% which draws 10A of current.

The team's mission will be to vertically touch and go on each landing point. First, an efficient velocity for maximum range was estimated using ecalc estimation tool. It was assumed that the maximum range possible is around 10 mph and yields mixed flight time of 9 minutes 50 seconds [3].

Flight duration based on battery consumption is calculated:

$$\frac{battery\ capacity(Ah)}{6 * current\ draw\ (A)} * \frac{60\ min}{1\ h} = flight\ time\ (\text{min})$$

Based on the manufacturer's specification, the current draw for a mixed flight condition is (55% throttle) ~ 10 A per motor [5]. With the propulsion system selected, a total of 9 min can be attained for a mixed flight condition. The analysis assumed the average speed to be 15 miles per hour, as maximum range with reasonable pace was achieved at this speed. The estimated time for one complete lap with 15 miles per hour is compiled in table 3.

Table 3: Flight Paths and Estimated Time

Flight Route	Distance (ft)	Time (seconds)
VTOL zones ascend	5ft ascend	5
VTOL zone to pad 1 flight	275 ft flight	(275 ft) / (22 ft/s) = 13
Pad 1 vertical takeoff/land	5ft descend & ascend	7
Pad 1 to pad 2 flights	389 ft flight	(389 ft) / (22 ft/s) = 18
Pad 2 vertical takeoff/land	5ft descend & ascend	7
Pad 2 to pad 3 flight	550 ft flight	(550 ft) / (22 ft/s) = 25
Pad 3 vertical takeoff/land	5ft descend & ascend	7
Pad 3 to VTOL zone flight	275ft	(275 ft) / (22 ft/s) = 13
VTOL zones descend	5ft descend	5
One Lap		100

Design Definition

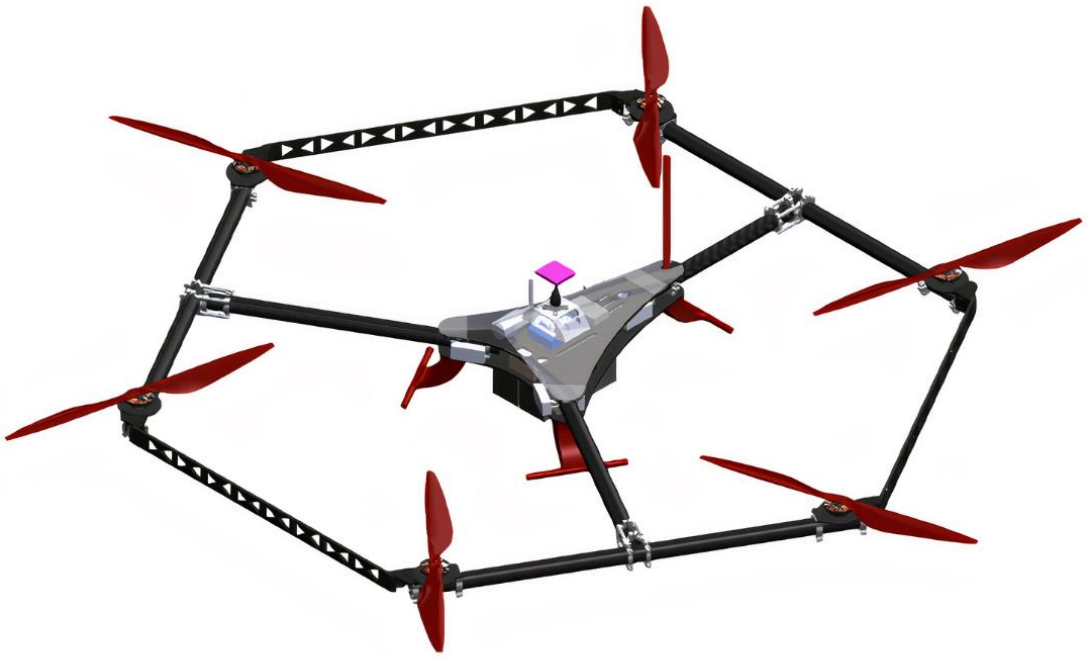

Figure 7: Isometric View of Aircraft in Vertical Flight

Airframe

The hexacopter consists of a carbon fiber body with an aerodynamic triangular fuselage. The inside of the fuselage consists of a plate with space allocated to mount avionic components. The shape of the hood does not allow for downward forces to act upon the airframe with a maximum forward flight tilt angle of 15 degrees. The outside corners of the fuselage are rounded and lead to three T-shaped arms. The T-shaped arms allow for minimal components coming off the fuselage, thus reducing weight. The T shaped arms are a hollow carbon fiber pultruded tube shaped like a T with mounting holes for the motors on each end. In order to reduce vibration, Delrin Trusses are added between the motor bearing tubes.

Motor

The T-Motor's Antigravity MN5008 was selected for the hexacopter. The motor measures 2.20 inches in diameter and 1.25 inches in height. The unit is rated at 340 kV, and it draws a maximum current of 35 A with an internal resistance of 55 mΩ. The motor generates 3.4 lb. of thrust at 50% throttle and 6.5 lb. of thrust at 75%. Equation (3) below calculates that the motor has a 0.0210 lb/W efficiency ratio at 50% power [5].

$$\frac{Motor\ Thrust}{Watt} = \frac{3.40\ lb}{162\ W} = 0.0210\ \frac{lb}{W} \quad (3)$$

Propeller

The hexacopter utilizes the TM-CFX-18x6.1 propellers and the specifications are listed in Table 4.

Table 4: TM-CFX-18" x 6.1" Propeller Specifications

TM-CFX-18X6.1				
Diameter & Pitch	18"x6.1"		Optimum RPM	3000-6000 RPM/min
Mass	0.0025±0.0001 oz		Thrust Limitation	18.1 lb.
Material	Carbon Fiber		T-MOTOR Series	2 blades-integrated

Electronic Speed Controllers (ESC)

The ESCs used for the aircraft are the APD F-Series 40F3. These ESCs each weigh 0.106 oz and provide 40 Amps continuous current, greater than the maximum motor draw of 35 Amps. All six of these ESCs receive Pulse Width Modulation (PWM) signals from the flight controller to regulate the power delivered.

Batteries

The batteries used for the propulsion system are Tattu 6S lithium polymer batteries. The configuration utilizes two of these batteries in parallel, which provides the system with a total capacity of 9000 mAh. A shunt plug will be installed in series between these batteries, and if necessary, the power distribution board that can quickly shut off the power to the motors. The battery used to power the flight controller and sensors is the Tattu 2S lithium polymer battery. This battery is more compact as the system it powers only needs a maximum of 5 volts. The specifications for the batteries are shown in Table 5.

Table 5: Propulsion and Flight Control Battery Specifications

Propulsion Battery			**Flight Control Battery**	
Tattu 6S 4500 mAh LiPo			Tattu 2S 550 mAh LiPo	
Cells	6		Cells	2
Discharge Rating	120C		Discharge Rating	95C
Amperage hour	4500 mAh		Amperage Hour	550 mAh
Watt Hours	99.9		Watt Hours	4.07
Mass	1.55 lb.		Mass	1.111 oz

Communication (Receiver, Telemetry)

The aircraft receiving device is the Graupner GR-12L SUMD Receiver, which provides bidirectional communications between the radio transmitter and the aircraft through 2.4 GHz bandwidth. The serial receiver is a digital package, offering direct connection to the flight controller with low latency control (3ms) for a high-performance receiving system. The receiver is compatible with a Graupner MZ-24 pro transmitter and provides up to 16 channels for control surfaces.

A 915 MHz telemetry radio connects directly to the flight controller and communicates with the ground station to provide navigation. It has the ability for autonomous mission planning, finding the precise location of the aircraft, and recording flight logs that can be analyzed later.

Flight Controller and Software

The open-source autopilot system PX4 was utilized as the firmware for the flight controller. The mRo Control Zero H7 OEM with a carrier board was selected as the flight controller. PX4 provides hardware support and a software stack for unmanned aircraft systems. PX4 consists of two main layers: flight stack and middleware. The flight stack includes an estimation and flight control system while middleware includes a general robotics layer. Flight controls and mission planning for the aircraft were performed using the ground control station QGroundControl. The 500mW mRo 915MHz Radio Telemetry was used to communicate between the aircraft and the ground station.

Predicted Mission Performance

Preliminary mission performance calculations were performed using the eCalc multicopter calculator [3]. The flight time and power required during flight were predicted using the information about the propulsion sub-systems as shown in Figure 8. Comparing all 15 configurations, the final configuration has an estimated flight time of 10 minutes and a hover time of 16 minutes. The configuration has a 3.5 thrust-to-weight ratio and operates at 87% efficiency at maximum thrust. The maximum speed of the hexacopter is 42.9 mph and has an estimated range of 1.87 miles. At optimum efficiency the motors draw 18.80 A at 21.11 V. At maximum efficiency, they draw 35.41 A at 20.14 V.

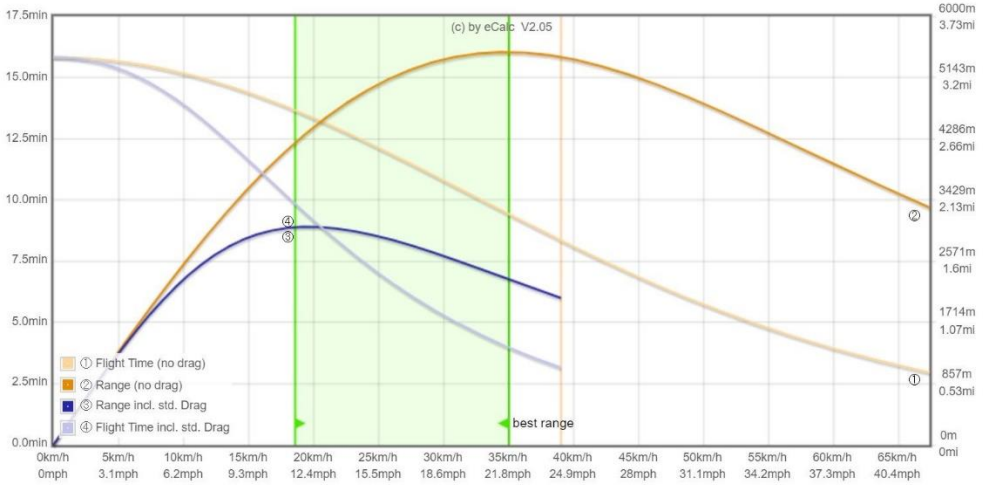

Figure 8: Range and Endurance with Standard Drag

Lift, Drag, and Stability

The thrust produced from the aircraft's propulsion system was estimated to determine the aircraft's lift capabilities while hovering. It was assumed that a thrust equivalent to the weight of the aircraft is sufficient to hover the aircraft. It was also assumed that the lift force is solely generated by the propellers for this calculation, so the estimate of the thrust required to maintain trimmed flight was deemed to be equivalent to the lift force. Before finding an estimate for the thrust required, the fuselage parasitic flat-plate area, f, must be determined using Equation (4) below [6].

$$f = \sum_{n} C_{D_n} S_n \tag{4}$$

S_n is the wetted area of the component and C_{D_n} is the parasitic drag coefficient. Rather than computing the flat-plate area on a per-component basis, it was computed as one entity. The wetted surface area for the entire aircraft was estimated in SolidWorks to be 13.73 ft^2 and the parasitic drag coefficient was estimated to be 0.0464. It should be noted that the parasitic drag coefficient was derived from the total drag coefficient in a study on UAV's simulated aerodynamics [7]. Typically, in a case of equilibrium flight, the thrust will be equal to the weight of the aircraft. However, the presence of vertical drag, due to the rotor's slipstream velocity requires an additional thrust to overcome the drag. Integrating the simple momentum theory to evaluate average velocity in rotor slipstream, the total thrust required is found in Equation (5) below [6].

$$T = \frac{W}{1 - \frac{f_v}{A}} \tag{5}$$

f_v is the equivalent drag area for a reference area S_{ref} and A is the disk area. The wetted area for the entire aircraft is used for the reference area, so $f_v = f$. The disk area for one propeller was computed and multiplied by 6 to account for all propellers on the aircraft. The equivalent disk area is 10.6 ft^2. The vertical drag can be estimated by subtracting the aircraft's weight from the estimated thrust required, so it can be determined that the estimated vertical drag is 0.96 lb. [6]. Multicopters are inherently unstable, and it requires a flight controller to perform safe and stable maneuvers. Within each flight controller, multiple control architectures, such as rate controller, position controller, and velocity controller, exist that help in stabilizing and improving the performance of the aircraft. PX4 uses a traditional PID (Proportional—Integral—Derivative) controller that requires an optimized set of gain values. A well-tuned PID control algorithm within the flight controller will be used to actively stabilize the aircraft, and the team plans to iteratively analyze the step responses plot to achieve optimal PID gain values during subsequent flight tests. Parameters such as rise time, steady state error, and maximum overshot will be analyzed to optimize the stability and performance of the aircraft.

Drawing Package

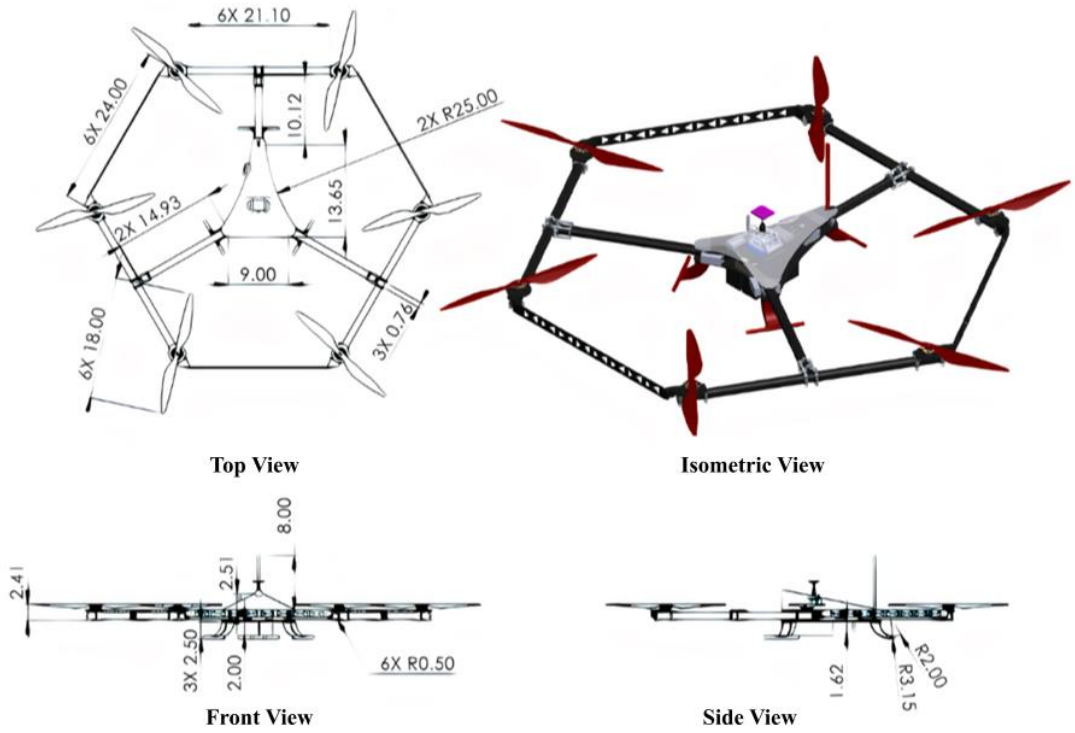

Figure 9: Engineering Drawings of Aircraft (Unit: Inches)

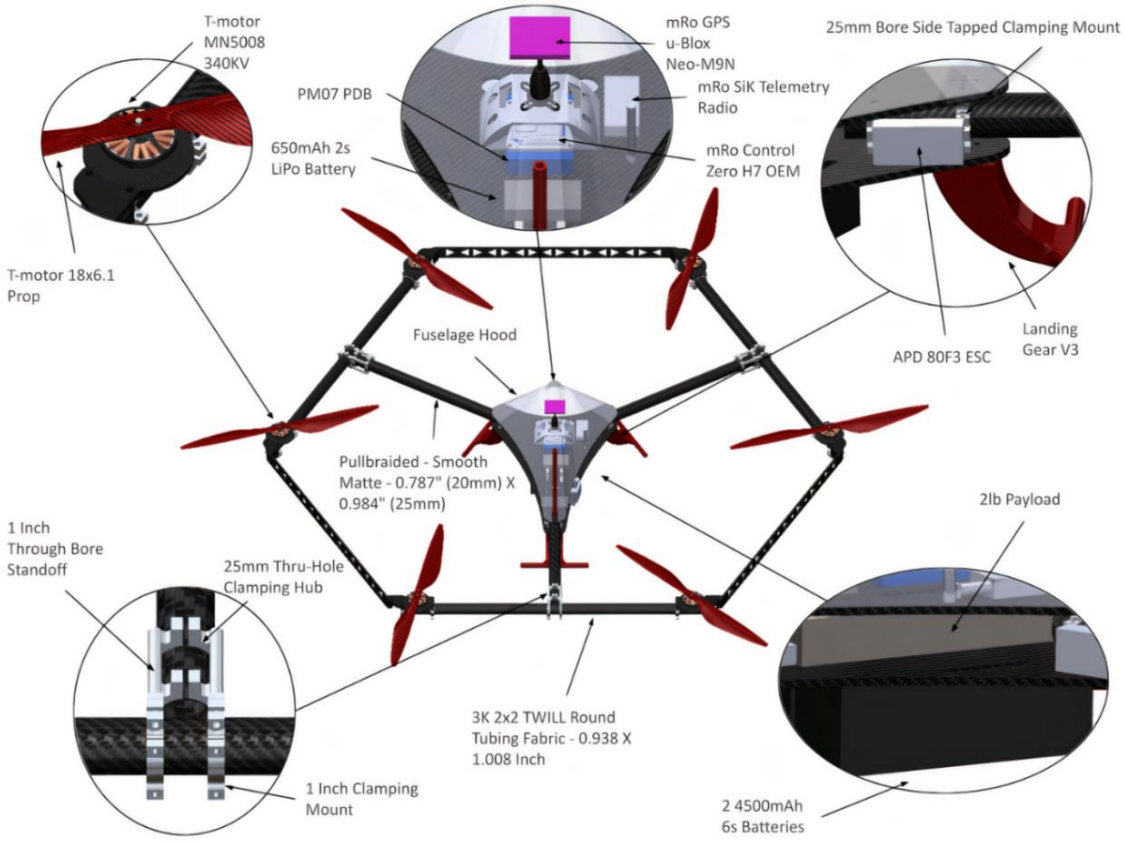

Figure 10: Structural, power, and avionics layout with callouts

Fabrication Methods

Manufacturing Processes

All main components of the aircraft are designed and fabricated at the Ohio State University. The manufacturing processes investigated are all available on campus. Resources such as vacuum bag systems, laser cutters, mills, CNC routers, and 3D printers allowed for a wide range of process to be investigated and down selected. Buckeye Vertical has members trained to use all equipment to allow for safe and proper use. Material selection was based off each component's design needs to allow for the on-time completion of the most effective aircraft. The tables below detail the selection of parts and display the selected materials and fabrication methods for each major component.

The process of wet layups and vacuum bag compression was examined in detail by the team. This process enables the ability to maximize the potential of composites by having the ability to interchange them when layering. The benefits of carbon fiber and Kevlar were examined in further detail, due to their diverse strengths and weaknesses. Carbon fiber is known for its lightweight and high Elastic Modulus while Kevlar has a tough, impact resistant structure with about half the strength of carbon fiber. Combining these two fabrics would allow for a part that would be stiff, while still having the ability to resist impact of load are applied. Materials such as fiber glass would create a part that would be strong and stiff, but still allow signals for avionics components to communicate through the material. Additive manufacturing is a process that allows for complex 3D shapes to be manufactured conveniently in a short amount of time. For additive manufacturing, the tradeoff between structural integrity and shape complexity is very important. 3D printed parts should be used when creating a non-loaded parts requiring 3D shapes. Infill densities and layer orientations can be modified to fulfill certain part requirements. Loaded parts will require a higher infill percentage and the layers to be printed perpendicular to the direction of the load. PLA+ filament can provide the part with a structural body. TPU filament can be used to soft mount motors to reduce vibrations within the aircraft.

Material Selection

The aircraft's material was determined based on a study of material strength, weight, and cost. The three materials considered and evaluated were garolite, carbon fiber, and Delrin. After analyzing stress tests in SolidWorks along with other material properties, it was determined that all 3 materials would be structurally sound for the applications on the aircraft. While carbon fiber is stronger than garolite and Delrin, other factors such as manufacturability, cost, and weight all played a factor in deciding to use Delrin for the fuselage plates.

Table 6: Investigated material specifications

Material (3/16" Thick)	Cost/Sq. Ft.	Density (lb/in^3)	Tensile Strength (psi)	Flexural Strength (psi)	Compressive Strength (psi)
Delrin Homopolymer	$18.75	.051	11,000	13,000	16,000
Garolite G10	$53.25	.074	55,000	61,000	75,000
Carbon Fiber	$114.48	.062	125,000	134,000	148,000

Final Manufacturing Process

Table 7: Final part materials and fabrication processes for airframe construction

Part	Material	Fabrication Process
Landing Gear	PLA+, Carbon Fiber, Kevlar	Additive Manufacturing, Wet layup, Followed by Vacuum Bag
Fuselage Hood	PLA+, Fiberglass	Additive Manufacturing, Wet Layup, Followed by Vacuum Bag
Fuselage Plates	Delrin	Laser Cutter
Carbon Fiber Tubes	Pultruded, 2x2 Twill weave Carbon Fiber Tubing	Table Saw
Motor Mounts	Delrin	Laser Cut
Motor Soft Mounts	TPU	Additive Manufacturing
Truss Mounts	PLA+	Additive Manufacturing
Truss	Delrin	Laser Cutter

Supplier parts were acquired as stock and were fabricated at the team lab. Carbon fiber tubes arrive as set lengths and are cut to the proper dimensions using a bandsaw. Delrin arrives as a 24"x48" sheet and is cut using a laser cutter to the shapes required. Carbon fiber, Kevlar, and fiber glass arrive as cloth, with pieces of the cloth being cut as needed. PLA+ and TPU arrive as a roll of filament to utilize with a 3D printer. The hexacopter was manufactured and assembled at Bolz Hall, a facility at The Ohio State University. Composite parts were constructed using a 3-step process. First, the mold is created through an additive manufacturing process, followed by detailed filing of the mold to ensure proper contact and adhesion of the epoxy resin. After proper filing procedures are completed, a wet layup is created using

layers of carbon fiber, Kevlar, and fiberglass. After ensuring all excess epoxy resin was removed, the wet layups are closed in a vacuum bag and left for 24 hours.

The assembly process was a very meticulous process requiring high level precision and accuracy. This process started by marking distinct clamp locations on the carbon fiber tubes using a caliper. Three individual T-Arms were assembled using precise markings and clamp hubs. These arms were subsequently mounted using clamps to the central fuselage plates while ensuring the measurements were followed precisely. At the completion of the assembly, an electric level is used to ensure that all mounts are equally level. At the completion of the level check, a string is taken from the center of the drone to ensure that all motors are equally spaced to ensure the location of center of mass.

Test Plan

It is essential to initially focus on vibration characteristics since most aircraft configurations are susceptible to vibration from high-power motors which restricts their performance. The resulting high frequency oscillations and noises adversely affect the efficiency of the aircraft. PX4 flight review – a web-based flight analysis tool – was utilized to visualize the flight performance of the aircraft. One of the graphs generated in the tool is the acceleration power spectral density, a 2D frequency plot showing the frequency response of the raw accelerometer data over time. The goal of the test plan is to restrict the acceleration power spectral density vibrations to a frequency of less than 80 dB. In order to appropriately address the vibration issues, the aircraft first had to be test-flown to collect data from each direction of movement. It was flown three feet above the ground to complete basic maneuverability tests and assess the vibration level. Once the aircraft had stabilized, the pilot produced slight roll, pitch, and yaw maneuvers using the remote controller for one minute. After conducting these movements, the aircraft landed, and a log file was extracted from the flight controller. The actuator control Fast Fourier Transform (FFT) was also accessed to examine high-intensity vibration frequencies. The chart shown in Figure 11 shows which regions of frequency needed attenuation. Depending on the results from the data, a structural or software-based solution would be implemented to address the issues

The tuning process of the flight controller was started once a satisfactory vibration response was achieved. Once the vibration in the airframe was attenuated through iterative potential solutions, the gains on the PID controller were tuned to maximize stability and controllability. PX4 firmware uses a traditional PID control algorithm. The tuning of the PID controller ensures faster and more precise responses from the pilot's input. The step response plot for each of the aircraft axis provided by the PX4 flight review was utilized to analyze the responsiveness. A threshold of rise time less than 0.15, and a maximum overshot of 0.5 were selected based on the first few flight tests of the aircraft. Here, the rise time refers to the time it takes the system to reach 90% of its setpoint.

After the assumed performance parameters of control and stability were met, a flight test to acquire flight time, speed, and the number of laps was conducted. Hover flight tests were conducted with minimum and incremented payload to compare to flight times and performance. Tests for flight speed and number of laps possible are conducted simultaneously as they dependently affect the flight performance. For the autonomous flight plan, a quadcopter was utilized to ensure the safety of the actual aircraft. Small mission plans using position based setpoints were created, and an iterative process was performed to set the velocities, trajectories, and mission time. During the flight path test, the team also observed any altitude changes, landing spot precision, ascending, and descending speed. A replica of the mission plan provided by the VFS was referenced to create a final mission script for the aircraft.

Flight Test Results

From the first prototype design, high vibrations and oscillations were observed during flight tests as shown in Figures 11-13. The team replaced the center beam on the T-beam with a thicker beam to decrease angle twist, further reducing vibration. There were improvements in the vibrations, but the results were not yet satisfactory. The aircraft had apparent flexing on the T-beam design, so to reduce general vibration and resonant vibration mode, the team incorporated a truss between two free motor ends to make a stiffer frame. The result of this improvement was that the aircraft exhibited only two resonant vibration modes each at 60 Hz and 90 Hz shown below on Figures 11 and 13.

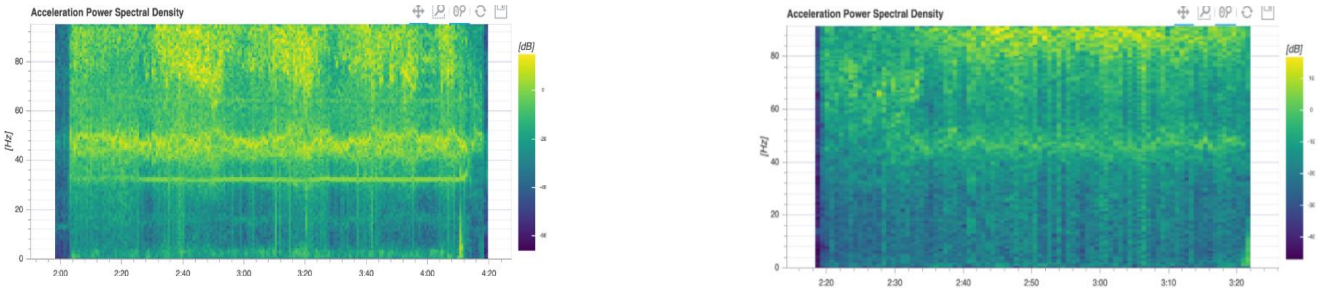

Figure 11: Comparison of Acceleration Power Spectral Density before and after vibration damping

The first iteration of the tuning was performed using the PX4 auto-tuning procedure. The innermost loop of the control architecture, rate controllers, were auto-tuned and flight tested. Manual changes in the PID gains were performed in later iterations to improve the response of the aircraft. The step responses plot of pitch rate before and after tuning is shown in Figure 12. The team plans to perform further iterations to tune the aircraft, such that the step responsiveness of the aircraft is critically dampened.

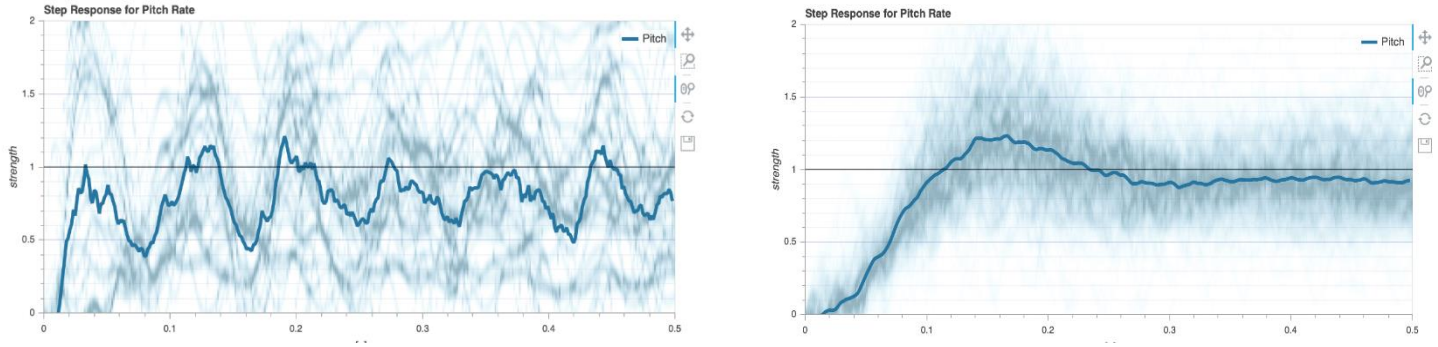

Figure 12: Comparison of step responses of pitch rate before and after tuning

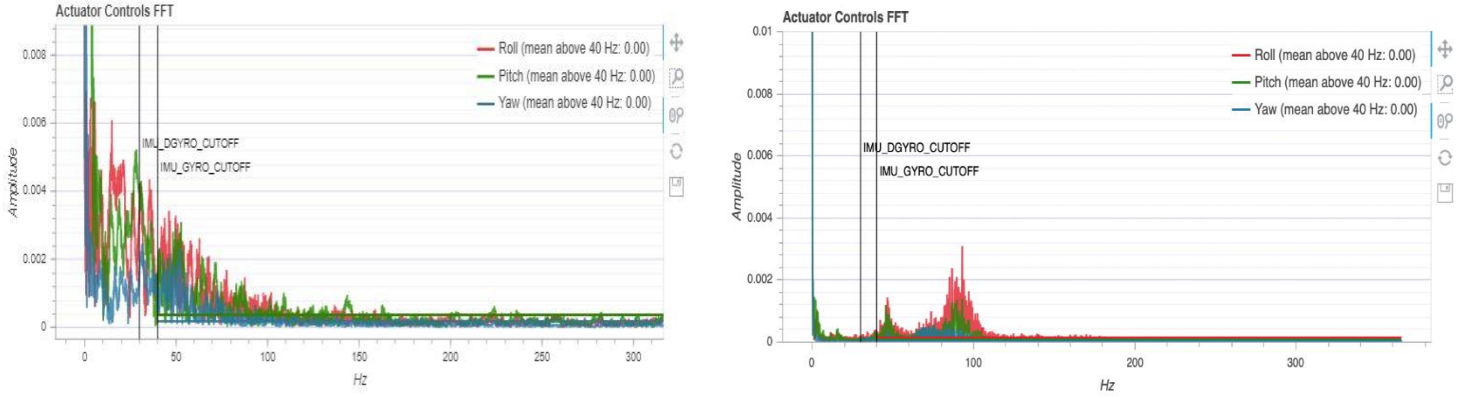

Figure 13: Comparison of Actuator Controls FFT before and after vibration damping

After the vibration damping with truss and stiffer beam, the vibrations were subdued and only resonant modes on 60 Hz and 90 Hz were visible, rather than high amplitude of low frequency band ranging from 0 Hz to 100 Hz as shown on figure 13.

Because static motor thrust tests are close but not accurate, the team conducted power usage from hover tests to demonstrate the real-world test. The aircraft weighed 11 lb. without payload and drew an average of 13 amps consistently during the hover flight. This yields efficiency of 0.0367 lb / W at 40% throttle from our test, compared to the manufacturer's specification of 0.0248 lb / W. The optimum payload and airframe weight was selected based on an iterative process as shown in Table 8. Compared to the estimation from eCalc calculator, the aircraft was consistently able to fly for more than 10 minutes, however the vibrations are likely still reducing its performance.

The team plans to perform further iterations to minimize the airframe weight and maximize the payload weight. The first hover flight test results without payload yielded about 20 minutes. With a 2 lb. payload attached, the aircraft hovered for 15 minutes 2 sec. During the mock-up forward flight test with the payload, the aircraft flew for 12.5 minutes, simulating take-off, hover, forward and backward flight, and landing 4 times.

Table 8: Flight Time vs. Total Weight of the aircraft

Airframe Weight (lb.)	Payload Weight (lb.)	Total Weight (lb.)	Flight Time
11	0	11	20 min 10 sec
11.5	0	11.5	18 min 30 sec
11	2	13	15 min 2 sec
11.5	2	13.5	14 min

References

[1] "Hexacopter vs. Quadcopter: The Pros and Cons." *Skilled Flyer*, 3 Nov. 2019, https://skilledflyer.com/hexacopter-vsquadcopter/.

[2] C.Ampatis and E. Papadopoulos, "Parametric design and optimization of multi-rotor aerialvehicles," 2014 IEEE International Conference on Robotics and Automation (ICRA), 2014, pp. 6266-6271, doi: 10.1109/ICRA.2014.6907783.

[3] Mueller, M. (n.d.). *XCOPTERCALC - multicopter calculator*. eCalc. Retrieved from https://www.ecalc.ch/xcoptercalc.php.

[4] Johnson, L. (2020, November 8). *How to calculate the force of a falling object*. Sciencing. Retrieved December 7, 2021, from https://sciencing.com/calculate-force-falling-object-6454559.html.

[5] *Antigravity MN5008 KV340*. T-MOTOR Store. (n.d.). Retrieved from https://store.tmotor.com/goods.php?id=999.

[6] Leishman, J. G. (2017). Principles of helicopter aerodynamics. Cambridge University Press.

[7] Raimundo Felismina, Miguel Silva, Artur Mateus, and Cândida Malça, "Study on the aerodynamic behavior of a UAV with an applied seeder for agricultural practices", AIP Conference Proceedings 1836, 020049 (2017) https://doi.org/10.1063/1.4981989

[8] Lofland, RA. "Composites 101 Workshop." https://www.aerodefevent.com/wp-content/uploads/2017/03/AeroDef-2017-Composites-101-Workshop.pdf.

[9] "PX4 Autopilot User Guide." PX4 User Guide, 2020